Research Journal of Pharmaceutical, Biological and Chemical Sciences

Equilibrium, Kinetic and Thermodynamic Studies for the Adsorption of P-Xylene by Graphene Nanosheets: Comparison with Carbon Nanotubes.

Mohammad T Raad[1, 2,] Malak Sayed Hassan[1, 2], Akram Hijazi[1, 2] *, Mounir Kassir [1], Hussein Medlej[3], May Issa [1, 3], and Mortada Srour [1, 2] *.

[1]Doctoral School of Science and Technology, Research Platform for Environmental Science (PRASE), Lebanese University, Lebanon
[2]Department of chemistry, Faculty of Sciences, Lebanese University, Hariri Campus, Hadath, Beirut, Lebanon.
[3]Department of environment, Faculty of agriculture, Lebanese University, Beirut, Lebanon.

ABSTRACT

In this study, Graphene nanosheets (GNS) were adopted as an adsorbent to study their characterizations and adsorption performance for p-xylene in an aqueous solution. Adsorption in a batch process was conducted to study the effect of initial concentration and contact time. Experimental data of adsorption were best followed by the Langmuir model for isotherm and pseudo-first order model for the kinetics. In the kinetic studies, it was observed that the process comes into equilibrium after 180 min and the maximum percentage removal was approximately 81 %. As a result, GNS displayed high affinity to p-xylene molecules, dominated by the π−π interactions of electronic density in the aromatic rings to the flat surface. The thermodynamic analysis indicated that the uptake of p-xylene by the adsorbent was physical, spontaneous, endothermic and favorable at higher temperatures. A comparative study on the p-xylene adsorption revealed that, GNS exhibited better adsorption capacities than carbon nanotubes.
Keywords: adsorption; graphene nanosheets; isotherm; kinetics; p-xylene;

*Corresponding author

INTRODUCTION

Petrochemical wastewater treatment constitutes a big challenge for research community due to its complex mixture of hydrocarbons. Characterization of wastewaters from two different petrochemical companies was presented and identified a large number of phosphorous, nitrogen, sulfur, oxygen-containing compounds as well as aliphatic and monocyclic or polycyclic aromatic hydrocarbons, including benzene, toluene and xylene aromatic compounds (BTX) [1]. These compounds are extremely toxic, presenting chronic toxicity even at low concentrations. Commercial xylene is a mixture of isomers that usually contains about 40-65% m-xylene and up to 20% each of o-xylene, p-xylene and ethyl benzene. This mixture is the most important product of all petrochemical industries. It has been classified as priority pollutant, which can represent a threat to the environment and to human health due to its toxic properties [2]. Among xylene isomers, the separation of p-xylene, $C_6H_4(CH_3)_2$, the most valued isomer, is more important from the economic point of view [3]. P-xylene removal from aqueous solutions has been reported using different methods, such as adsorption [4, 5], advanced oxidation processes [6] and biological processes [7]. Each of these processes has advantages and disadvantages; however, adsorption offers a more efficient way to purify the effluent to a point where it is suitable for discharge into the environment. Conventional adsorption via activated carbon as adsorbents has been widely used in literature for this purpose [8]. Over the last 20 years, new members of the carbon nanostructure family arose, and more are coming. Graphene is the latest member of the carbon family and is believed to be one of the most interesting materials of this century [9]. Graphene and its composites offer utility in several applications due to its unique two dimensional natures, associated band structure, excellent mobility of charge carriers and high thermal conductivity [10]. Graphene nanosheets are two-dimensional, planar sheets of sp^2 hybridized carbon atoms packed in a hexagonal honeycomb lattice, and constitute basic building block of fullerenes, carbon nanotubes (CNT), and graphite [9]. The graphene sheets tend to stack together (π–π stacking) because of the strong van der Waals forces between the single layers [11]. Carbon nanotubes have been proven to possess good potential as adsorbents because they join relatively high specific surface area and uniform mesoporous diameter [12]. As compared to carbon nanotubes, GNS possess an open-layered structure that has a completely accessible adsorption surface for organic molecules [13]. Commercial production and industrial scale application of graphene nanosheets are expected to grow exponentially over next decades [14, 15], mainly due to its unique structural and physical properties and potentially low cost. It has been demonstrated that in addition to the hydrophobic effect, π–π interactions were responsible for the strong adsorption of organic molecules onto graphene-like materials [16, 17]. However, up to now, no investigation has been carried out on utilizing GNS as an adsorbent to remove p-xylene from wastewater. Such studies are still very limited in the literature. The main objective of this work is to evaluate the potential of a GNS for wastewater treatment contaminated with p-xylene. Equilibrium isotherms and kinetics as well as thermodynamic parameters are obtained using monocomponent p-xylene solutions and parameters will be obtained to understand the non-covalent π-π stacking interactions between the GNSs and aromatic organic molecules. Furthermore, a comparative study on the adsorption capacity of p-xylene with CNTs will be discussed.

EXPERIMENTAL

Chemicals

The employed p-xylene was analytical grade with > 98% purity and purchased from Merck Company. P-xylene solutions were prepared by dissolving appropriate volumes of p-xylene in distilled water. Ultrapure water was obtained using a Milli-Q system (Millipore, Bedford, MA, USA). The basic characteristics of p-xylene compound are presented in Table 1.

Table 1: Physical and chemical characteristics of DNT at 25 °C.

Compound	Molecular weight (g/mol)	Boiling point (°C)	Solubility in water (mg/L)	Density (g/mL)	Vapor pressure (Pa)
P-Xylene	182.134	300	200	1.52	0.02

Adsorbent

The adsorbent used was graphene nanosheets, (99.5%, Thickness 2-18 nm with less than 32 layers) with density equal to 1.9 ~ 2.2 g/cm³ at 20 °C. The microstructure and morphology of GNS were characterized by elemental analysis, BET specific surface area (BET-N_2), pore volume, X-ray photoelectron spectroscopy (XPS), Raman spectra, Scanning Electron Microscopy (SEM), Transmission Electron Microscopy (TEM), X-ray diffract meter (XRD) and Fourier transform infrared spectroscopy (FTIR).

Batch adsorption study

Equilibrium studies (effect of initial concentration)

Batch adsorption experiments were conducted in batch conditions using 100 mL glass bottles with addition of 30 mL p-xylene and 0.05 g of GNS. The glass bottles from the batch experiments were placed on a Multi-shaker (Model PSU20) and were stirred at 205 rpm at room temperature 20 °C. The solution samples were then allowed to settle and the supernatant was filtered and the remaining concentrations were determined by HPLC chromatograph. The amount of p-xylene adsorbed at equilibrium is commonly called the adsorption capacity, q_e. The q_e value can be calculated by Eq. (1):

$$q_e = (c_o - c_e)\frac{V}{m}$$

(1)

Kinetic studies (effect of contact time)

The adsorption kinetics was carried out in a batch system, similar to that in the equilibrium studies. Samples were collected at predetermined time intervals (in regular periods of time), up to 240 min total time and filtered.

The sorption capacity q_t of GNS was calculated using the Eq. (2):

$$q_t = (c_o - c_t)\frac{V}{m}$$

(2)

To determine the percentage of p-xylene removal, Eq. (3) is used:

$$\% \, removed = \frac{(c_o - c_e)}{c_o} * 100$$

(3)

Analytical methods

P-xylene concentrations were determined by high performance liquid phase chromatography-HPLC equipped with a SPD-10A VP UV/visible detector and LC-10AT VP pump. The reverse-phase column (Nucleosil C18, Bond Pack 4µm, internal diameter of 4.6 mm, length 150 mm) was operated at room temperature (20 °C). The mobile phase was prepared daily in proportions of 70:30 (methanol/Milli-Q water), and delivered at a flow rate of 1.0 mL/min in isocratic mode during 12 min and the wavelength of the UV absorbance detector was set at 254 nm.

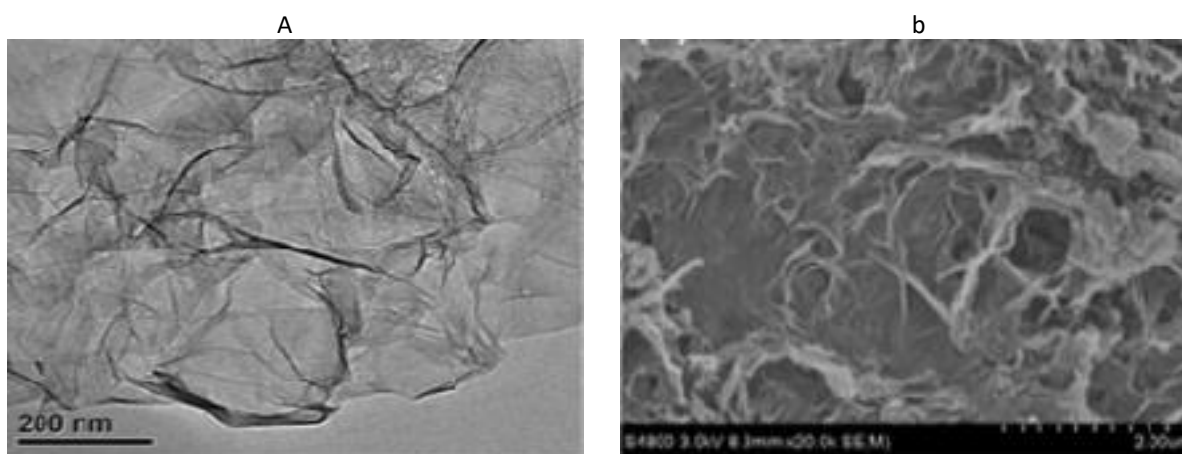**Effect of adsorbent dosage on the adsorption capacity**

To study the effect of adsorbent dose on removal of p-xylene, different amounts of GNS (0.01 to 0.1g) were taken and agitated with 30 mL of p-xylene solution for 10 h. The experiment was carried out in 100mL glass bottles. The flasks were placed Multi-shaker (Model PSU20) and were stirred at 205 rpm at 20 °C.

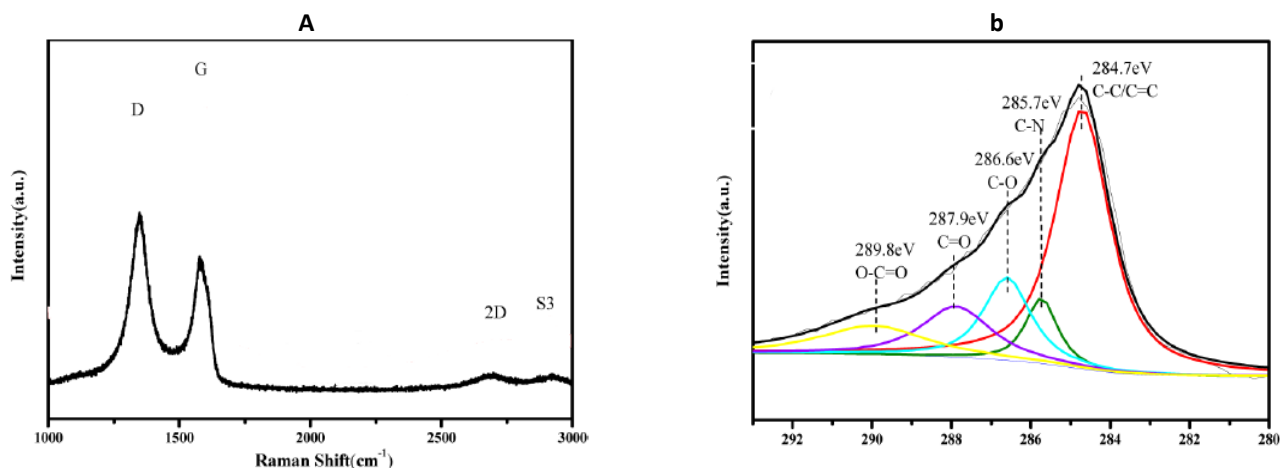## RESULTS AND DISCUSSION

Adsorbent characterization

The surface morphology of GNS was characterized through S-4800 Field Emission Scanning Electron Microscopy (FE-SEM) and JEM-2010 Transmission Electron Microscopy (TEM). The TEM and SEM images of GNS are presented in Fig. 1. The TEM image (Fig. 1a) revealed that GNS film was transparent and slightly aggregated with the wrinkles loosely distributed on the basal planes of GNS to form groove regions. However, CNT usually form an aggregated structure due to inter-molecular force. This nature of GNS can be also confirmed by the typical ripples present on the GNS surface (Fig. 1b).
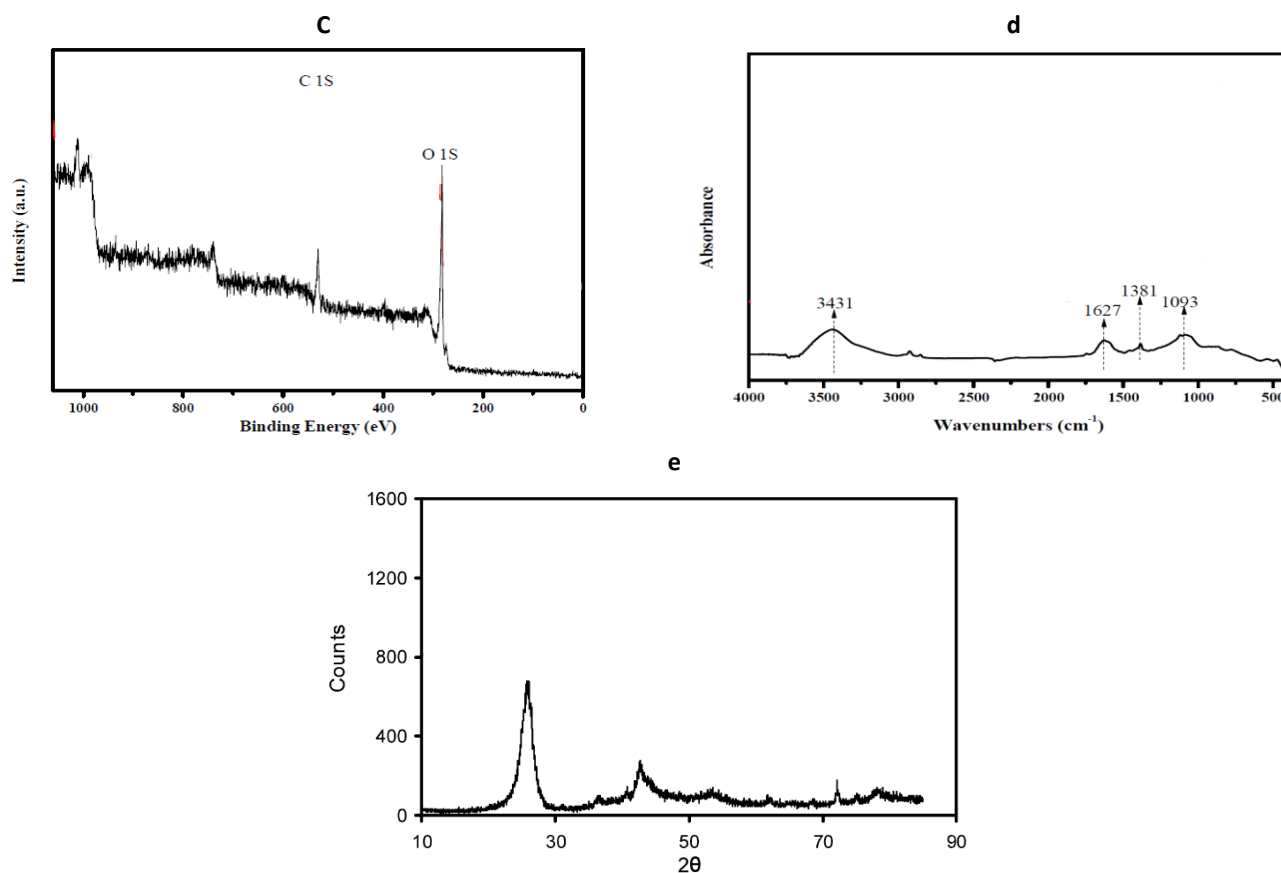
Fig 1: (a) TEM and (b) SEM images of GNS.

The structure information of GNS was evaluated by a Raman spectrometer. A Raman spectrum was obtained with a LabRamHRUV Raman spectrometer (JDbin-yvon, FR); the laser excitation was provided by an Ar^+ laser at a wavelength of 514 nm. In the Raman spectra, Fig. 2a, two prominent peaks at 1349 and 1582 cm^{-1} correspond to the D and G bands, respectively. The D band originates from the stretching vibration of sp^3 carbon atoms, which induces defects and disorders, whereas the G band originates from the stretching vibration of sp^2 carbon atoms, corresponding to the first-order scattering of the E_{2g} mode. Hence, the extent of carbon-containing defects of adsorbents can be evaluated by intensity ratio of D band to G band (I_D/I_G). The intensity ratio of the D band to the G band (I_D/I_G) of GNS is 1.28, is higher than those of commercially available CNT which is 0.68, documented in the literature (Kang et al., 2008). This indicates that the employed GNS possess more carbon-containing defects than the commercially available CNT.

Fig 2: Characterization of (GNS): (a) Raman spectra, (b) XPS spectrafor C 1s, (c) XPS of GNS in a wide scan, (d) FTIR spectra and (e) X-ray diffract meter (XRD).

C

d

e

The surface chemical analysis and surface functional groups were observed by X-ray photoelectron spectroscopy (XPS) and Fourier transform infrared spectroscopy (FTIR), respectively in Figs.2b, 2c and 2d. The XPS experiment was performed on a spectroscopy (XPS, PHI 5000 VersaProbe/Scanning ESCA Microprobe, ULVAC-PHI Inc) with a mono-cromatized Mg K⬜⬜(1253.6 eV) X-ray source with a resolution below 0.2 eV, and the C 1s peak spectra (Fig. 2c) were analyzed using XPS Peak 4.1 software. In Fig. 2b, deconvolution of the C 1s peak of GNS resolves to a main peak at 284.7 eV, which is attributed to the presence of $C=C$ / $C-O$ bands. The peaks at 286.6, 287.9, and 289.8 eV correlate to the carbon in $C-O$, the carbonyl carbon in $C=O$, and the carboxyl carbon in $O-C=O$, respectively. Although the C 1s spectrum of CNT shows the same functionalities compared with GNS, the O 1s peak of CNT is located at 532.9 eV, which is very increased, is associated with $C=O$ band, indicating that the surface of CNT is more hydrophilic than that of GNS, whereas the sp^2 hybridized zone on CNT is less than that of GNS. The surface functional groups of GNS were detected by a Fourier transform infrared ray (FTIR) spectrometer.

The FTIR spectra were recorded in the 4000-400 cm^{-1} region with a resolution of 4 cm^{-1} using a Bruker Vector 22 FTIR spectrometer. The FTIR spectrum of GNS was shown in Fig. 2d. The peak at 1627 cm^{-1} was assigned to the benzene ring $C=C$ stretching vibration. Only a few polar functional groups are existed on the surface of GNS in comparison to the CNT, and the surface of GNS is highly hydrophobic. Elemental analyses were conducted using an EA112 CHN elemental analyzer (Thermo Finnigan). The elemental composition of GNS (76.2% C, 1.03% H, 17.6% O and 5.17% N) was in agreement with the FTIR results. Structural support can also be assessed by XRD analysis. The crystal phase of GNS was characterized by a powder X-ray diffract meter (XRD, Mac Science Co. Ltd) using Cu K⬜ radiation (40 kV, 30 mA), Fig. 2e. Measurements of the samples were carried out in the range 2θ of 10°–85° at a scanning rate of 2° in 2θ min^{-1}. The XRD profiles are dominated by a peak at 26° that is characteristic of highly structured GNS, whereas a second peak is located at 42°. These peaks correspond to the periodicity between graphene layers and within a graphene layer, respectively. GNS demonstrate the strong presence of a graphitic phase due to the 2θ = 26° major peak. The broadness of the 2θ = 26° peak is indicative of a loss of crystallinity.

The Brunauer-Emmett-Teller (BET) nitrogen specific surface area of GNS was estimated by nitrogen adsorption-desorption at 77 K with a NOVA-2000E surface area (SA) analyzer. The BET specific surface area of

GNS was 392 m^2/g. The high SA may directly reflect the exfoliation degree of graphene materials compared to that of graphite (4.5 m^2/g) (Zhu and Pignatello 2005). The measured BET surface area was smaller than the theoretically calculated surface area (2630 m^2/g) for monolayer carbon structured GNS (Stoller et al., 2008), which should be related to incomplete exfoliation and aggregation during the sample preparation process. The values obtained in this study were in agreement with those reported for other graphenes in literature (Ramesha et al., 2011). The specific surface area of the graphene nanosheets measured with (BET-N$_2$) method, 392 m^2/g, was approximately two times of that for carbon nanotubes (186 m^2/g). Pore volumes were determined from nitrogen physisorption data at 77 K with (Micromeritics ASAP 2000 surface analyzer), and using the density functional theory (DFT) model, assuming a value of 0.164 nm^2 for the cross section of the nitrogen molecule. Although the aggregation characteristics may change when GNS is in water, the nitrogen adsorption isotherms indicated that these graphenes had similar distribution of mesopores (2–50 nm), and no micropores (<2 nm). The GNS had approximately 3-4 times higher pore volumes than CNT (1.39 cm^3/g), which may be attributed to their much less compact aggregate and bundle structures as compared to CNT. This fact was also in good agreement with the SEM observations (GNS seems to be more porous than CNT). It suggests that GNS have more amount of porosity than CNT in a mesopores. The pore volume from N$_2$ adsorption data behaves as expected, in the same manner as the BET surface area because mesopores are mainly responsible for the specific surface area.

Adsorption isotherms

Langmuir isotherm

The Langmuir isotherm is based on the assumption that adsorption takes place at specific homogeneous sites within the adsorbent, and there is no significant interaction among adsorbed species [18]. The adsorbent is saturated after one layer of adsorbed molecules is formed on the adsorbent surface. The Langmuir isotherm [19] is represented by Eq. (4):

$$q_e = \frac{q_{max} \, b \, c_e}{1 + b \, c_e} \tag{4}$$

Freundlich isotherm

The empirical Freundlich model [20] based on adsorption on a heterogeneous surface is given by Eq. (5):

$$q_e = k c_e^n \tag{5}$$

Sips isotherm

The Sips isotherm is another three-parameter isotherm that derived by combination of the Langmuir and Freundlich isotherms and is therefore also called Langmuir–Freundlich (Sips) isotherm. The Sips equation [21] is given by Eq. (6):

$$q_e = \frac{q_{max} \, b \, c_e^n}{1 + b \, c_e^n} \tag{6}$$

Fig. 3 contains plots of the fitted isotherms for p-xylene, along with the experimental data points. Although linear regression was frequently used to determine the most fitted isotherm, nonlinear method offered a better way to predict the equilibrium isotherm parameters. The determination of isotherm parameters here was done by nonlinear regression by using OriginPro, Table 2. The best fitting equation is based on the highest R^2 and the lowest χ^2. On evaluating the parameters shown in Table 2, the Langmuir isotherm expression provides the best fit; it is the most suitable model characterizing the adsorption of p-xylene. This means that the adsorption of the p-xylene onto GNS possibly occurred according to the conditions assumed in Langmuir model, that is, the adsorption is a monolayer phenomenon, and the adsorption sites are not identical to each other, resulting in different affinities between the solutes and the adsorbent. The high
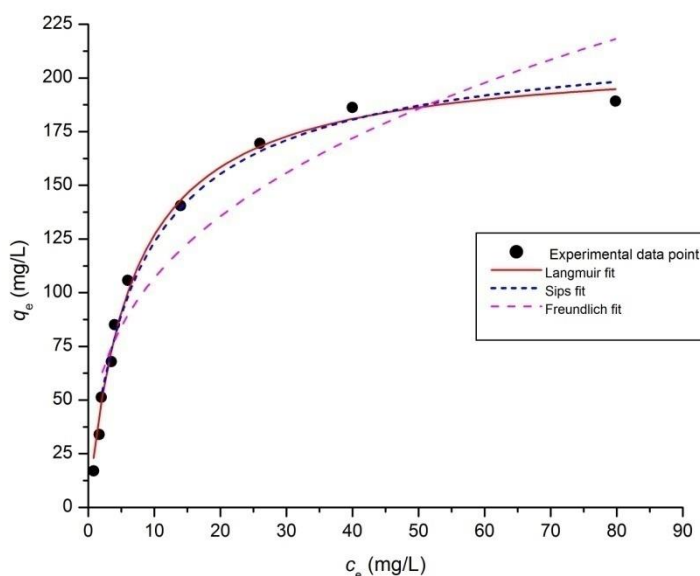
value of q_{max} for p-xylene, 211 mg/g, makes GNS a very promising and highly performing adsorbent for removal of p-xylene from aqueous solutions. Comparisons for q_e from this study with various adsorbents reported in the literature are given in Table 3. Under analogous conditions, the present graphene nanosheets showed better performance for p-xylene adsorption than do other adsorbents. Favorable adsorption of GNS compared to CNT was also dependent on physical properties such as the specific surface area and the porosity. It was consistent with the order of specific surface area and pore volume. This suggests that the graphene nanosheets are efficient adsorbents and they possess good potential for p-xylene removal in wastewater treatment.

Table 2: Isotherm modeling parameters related to the adsorption of p-xylene onto graphene nanosheets (nonlinear approach) at 20 °C.

Model	Parameters	P-Xylene
Langmuir	χ^2	34.07
	R^2	0.994
	q_{max} (mg/g)	211
	b (L/mg)	0.15
Freundlich	χ^2	466.1
	R^2	0.898
	k (mg/g)(L/mg)^n	48.39
	n	0.34
Sips	χ^2	58.76
	R^2	0.987
	q_{max} (mg/g)	202
	b (L/mg)^n	0.16
	n	0.88

Table 3: Adsorption capacity of this study compared with various adsorbents as reported in literature.

Adsorbent	Adsorption capacity (mg/g)	Conditions	References
Graphene nanosheets	211	pH 7, T: 20, S/L: 0.05/30, C0=25–100	This work
Single-walled carbon nanotube	77.5	pH 7, T: 20, S/L: 0.1/100, C0=10–100	[22]
Carbon nanotube	172.7	pH 7, T: 25, S/L: 0.06/100, C0=20–200	[23]
Activated carbon fiber	185	pH 7, T: 20, S/L: 0.5/40, C0=10–100	[10]

It is worth mentioning that, in the adsorption of aromatic compounds on graphene nanosheets in a liquid solution, there are two main types of interactions, namely electrostatic and dispersive interactions. Here, in the aqueous solution, p-xylene is in the molecular form; in this case, dispersive (π–π interactions) are predominant, mainly because of the attraction between the π orbital on the graphene nanosheets and the electronic density in the p-xylene aromatic rings (noncovalent π-π stacking interactions) [24], which is responsible for the physisorption of p-xylene on graphene nanosheets.

Kinetic models

For the interpretation of the kinetic data, a pseudo-first-order kinetic model Eq. (7) [25] and a pseudo-second-order kinetic model Eq. (8) [26] were used. In order to design a fast and effective model, investigations are made on adsorption rate. The nonlinearized form of the pseudo-first order equation (Lagergren) is generally expressed by Eq. (7):

$$q_t = q_{eq}[1 - exp(-k_{1,ads}\, t)] \tag{7}$$

and the pseudo-second order kinetic model is represented by the following Eq. (8):

$$q_t = \frac{q_{eq}^2\, k_{2,ads} t}{1 + k_{2,ads}\, q_{eq} t} \tag{8}$$

The initial adsorption rate ($r_{ads}(i)$) can be calculated from Eqs. (9-11):
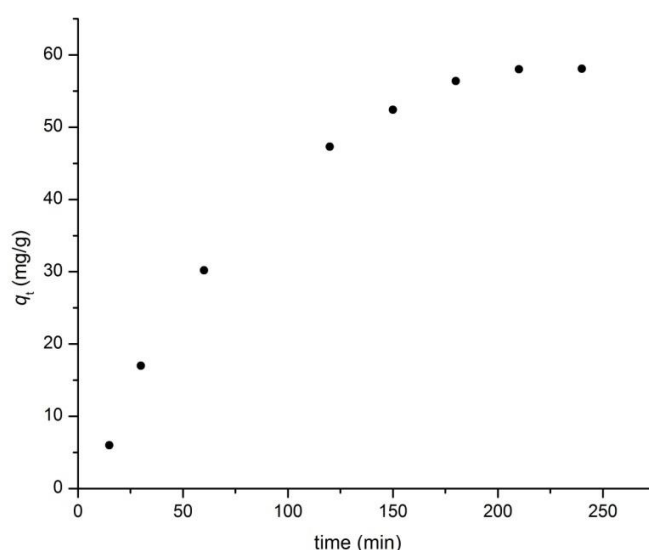
$$\left(\frac{dq}{dt}\right)_{t=0} = r_{ads}(i) \tag{9}$$

$$r_{ads}(i) = k_{1,ads} q_{eq} \tag{10}$$

$$r_{ads}(i) = k_{2,ads} q_{eq}^2 \tag{11}$$

for the pseudo-first-order (Eq. 10) and pseudo-second-order (Eq. 11) models, respectively. The effect of contact time on p-xylene adsorbed by GNS was studied and shown in Fig. 4. It can be seen that, the rate of adsorption was very fast in the first 15 to 145 min, then gradually slowed down from 145 to 170 min until equilibrium is reached. The fast adsorption may be due to the layered structure of GNS. Removal of p-xylene by the GNSs is faster at the initial stage and gradually decreases with time until saturation. This is attributed to

the diffusion of the p-xylene molecules into the internal pores, as those adsorbents have a high surface area and porosity. The GNS had approximately 3-4 times higher pore volumes than CNT, which may be attributed to their much less compact aggregate and bundle structures as compared to CNT. It suggests that GNS have more amount of porosity than CNT in a mesopores. The pore volume from N_2 adsorption data behaves in the same manner as the BET surface area because mesopores are mainly responsible for the specific surface area. In addition, the presence of acidic functional groups on the GNSs favor the specific interactions between π orbital on the carbon basal plane and the aromatic rings of p-xylene thus enhancing the adsorption. Moreover, as GNS contacts with p-xylene in the aqueous solution the adsorption occurs immediately as a result of the strong π−π interactions between GNSs and the aromatic organic molecules. With further increase in time, the diminishing availability of the remaining π-electron molecular assemblies and the decrease in the π−π stacking interactions, it takes a long time to reach at the equilibrium. Consequently, the adsorption rate becomes slower.

Fig 4: Effect of contact time on p-xylene adsorption at 20 °C.

Finally, the equilibrium states were achieved in almost 180 minutes within the considered experimental concentration range. Thus, although 180 minutes seem to be sufficient to reach at the equilibrium for the selected p-xylene concentrations, the isotherm experiments, time were extended for a total duration of 240 minutes to ensure a full saturation.

The pseudo-first order model provides a better fit to the experimental results based on highest R^2 and the lowest χ^2. The pseudo-first and -second order adsorption kinetic parameters were evaluated by nonlinear regression analysis by using OriginPro, and are presented in Table 4. The pseudo-first order model may be related to the occurrence of physical sorption, which may control the reaction rate [27], that confirms our aforementioned interpretation.

Table 4: Pseudo first and second order adsorption kinetic parameters from non-linear regression analysis

Pseudo-first order (Non linear)					
Adsorbate	q_e(mg/g)	k_1(min^{-1})	r_{ads} (i) (mg/g/min)	R^2	χ^2
P-Xylene	65.46	0.0101	0.675	0.994	2.97
Pseudo-second order (Non linear)					
Adsorbate	q_e(mg/g)	K_2(g/mg/min)	r_{ads} (i) (mg/g/min)	R^2	χ^2

| P-Xylene | 18.56 | 0.0012 | 0.413 | 0.9728 | 29.660 |

Thermodynamic Analysis

The thermodynamic parameters are calculated according to the Eqs. (12-14):

$$\ln(K) = \frac{-\Delta H^0}{R}\frac{1}{T} + \frac{\Delta S^0}{R} \tag{12}$$

$$\Delta G^0 = \Delta H^0 - T\Delta S^0 \tag{13}$$

$$K = \frac{[p-xylene]_{ads}}{[p-xylene]_{final}} = \frac{(c_o - c_e)}{c_e} \tag{14}$$

The values of (ΔH^0) and (ΔS^0) can be evaluated from the slope and intercept of the plot of $\ln(K)$ against $\frac{1}{T}$, Fig. 5. The calculated parameters are listed in Table 5. This process can be considered as physisorption. The negative values of Gibbs free energies (ΔG^0) indicate that the adsorption of p-xylene on the GNS is feasible and spontaneous and the positive value of enthalpy change (ΔH^0) confirms the endothermic nature of the present adsorption process.

Fig 5: Plot of $\ln(K)$ against $\frac{1}{T}$ for the adsorption of p-Xylene adsorption onto GNS.
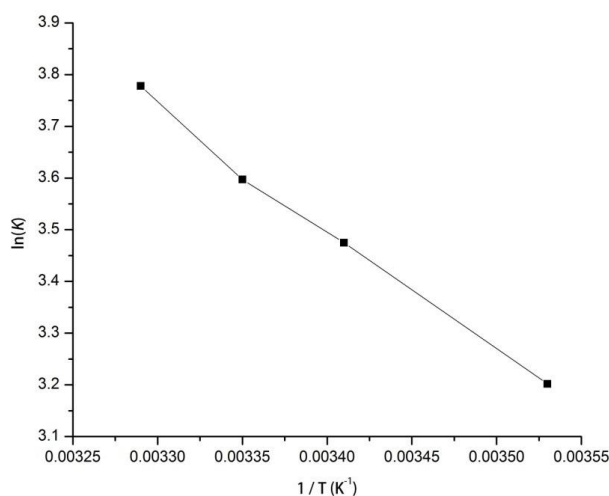

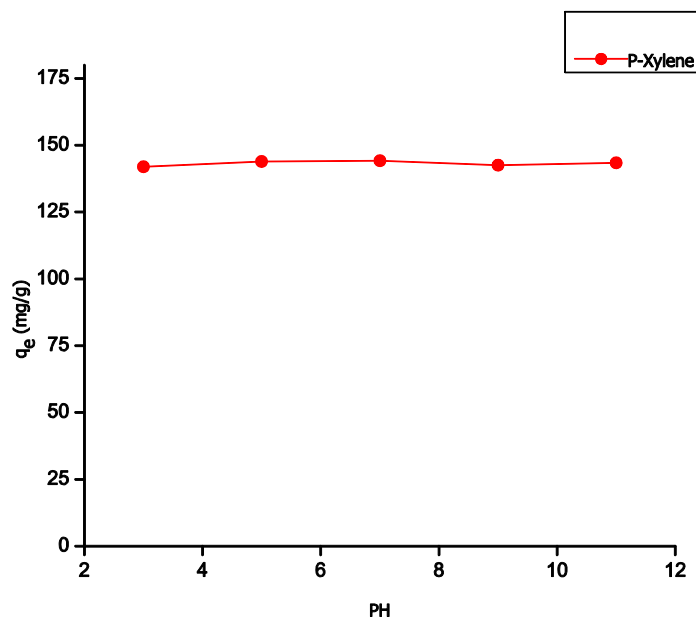**Table 5: Thermodynamic parameters of p-xylene onto graphene nanosheets**

ΔH^0 (kJ/mol)	ΔS^0 kJ/(mol K)	$-\Delta G^0$ (kJ/mol)			R^2
		283.15(K)	293.15(K)	298.15(K) 303.15(K)	
19.57	0.095	7.49	8.45 9.41	8.93	0.995

Effect of PH on the adsorption capacity

The effect of PH was studied for the PH range of 3 to 11 at a temperature of 20 °C. Fig. 6 shows the effect of PH on p-xylene adsorption via GNS. It is observed that the change in PH has insignificant effects on p-

xylene adsorption, reflecting high stability of GNS as p-xylene adsorbents in a wide range of solution PH and implying that p-xylene are in molecular forms during adsorption process and that ion-exchange doesn't play a part in p-xylene adsorption. The pH was adjusted at neutrality and controlled at 7 during the adsorption study. Water solubility of p-xylene was estimated 198 mg/L at PH 7.

Fig 6: The Effect of PH on the p-xylene adsorption via GNS at 20 °C.

Adsorption mechanism of p-xylene to GNS

Certain studies on the adsorption of organic pollutants to nanomaterials were attributed to the existence of high surface energy sites, such as defects, edges, and groove areas [28, 29] because molecules would initially occupy these sites with strong affinities. This suggested that in addition to the hydrophobic effect and π–π interactions, other adsorption mechanisms should also be considered. Furthermore, the intrinsic wrinkles on graphene nanosheets have been reported to lead to charge inhomogeneities in the charge distribution, and the wrinkles show concentrated charge with high chemical activity [29, 30]. Therefore, the relationship between graphene morphology and adsorption sites is investigated to further elucidate the additional mechanism. We hypothesize that the graphene surface crumples with low organic pollutants adsorption to the surface creating grooves with high adsorption energy sites. The high energy adsorption sites create a favorable adsorption until the "turning point" and at higher adsorption concentrations the surface morphology transforms leading to a more typical adsorption mechanism. The morphologies of GNS after adsorption were monitored by TEM. Because both experimental and theoretical studies have revealed that wrinkles have concentrated charge with high chemical activity, [29, 30] compared with the flat surface, the grooved regions are regarded as high surface energy sites.
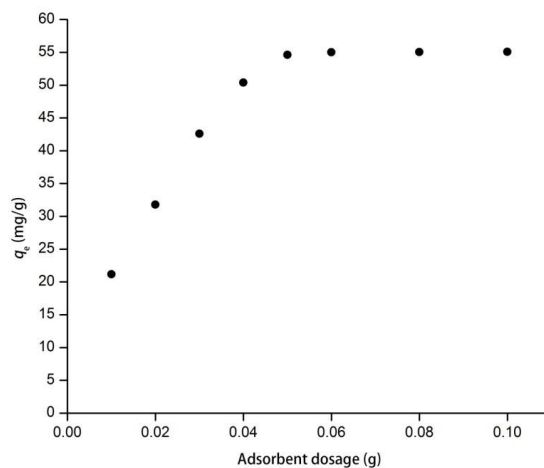
Generally, the intrinsic wrinkles are essential for the structural stability of single layer graphene [31, 32]. However, the degree of wrinkling will decrease with increasing stacking graphene layers [31], thus graphene can stack into 3D graphite with a flat surface. The sieving effect may play an important role in the adsorption because the accessibility of adsorption regions on graphene for molecules with distinct sizes was different.

Effect of adsorbent dosage on the adsorption capacity

The result of the experiment performed to study the effects of adsorbent dosage on p-xylene removal was shown in Fig. 7. Clearly, the removal turnover of the p-xylene by the GNS was increased parallel to an increase in the adsorbent dosage. Besides a prompt increase was observed at adsorbent dosages ranges
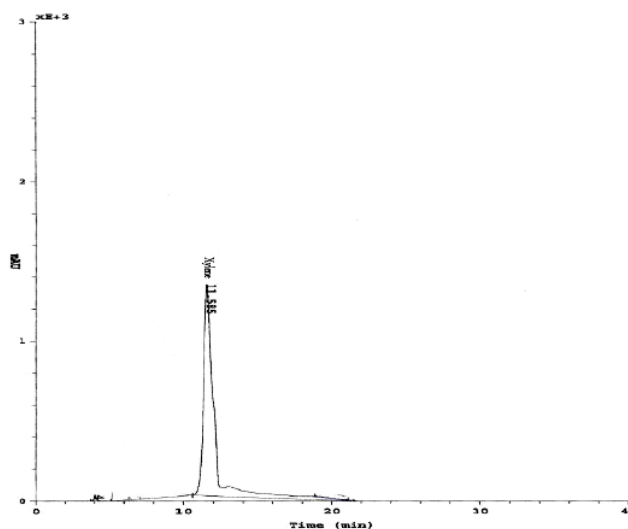
between 0.01 and 0.05 g, a plateau was seen at the range between 0.05 and 0.1 g. Further increase in the adsorbent dosage above 0.05 g had meager effect on the increase in removal efficiency of p-xylene. This may be corresponded to the formation of aggregates at higher solid/liquid ratios or to sediment of particles [33].

Fig 7: Effect of the adsorbent dosage for p-xylene adsorption on GNS at 20 °C.

The HPLC method required the use of methanol as a component of the mobile phase. To determine optimum ratio of methanol-water for the mobile phase of HPLC, different ratios of these solutions were used to analyze p-xylene (volatile organic compound). As expected, the higher the methanol content of the mobile phase, the lower the retention time became. The results indicate that a methanol-water ratio 70:30 has the best resolution for high peak area and retention time. The retention time for p-xylene was 11.58, Fig. 8. The result of current study was indicated that HPLC-UV method proposed here can be employed as a alternative for separating and determining p-xylene in occupational environments. HPLC determination of p-xylene was applicable to real samples because its sensivity was lower than the thershold limit recommended by the American Conference of Governmental Industrial Hygienist (ACGIH) for an 8-hour workday. As a result, the use of the mobile phase has shown its potency for the adsortion of p-xylene from aqueous solution.

Fig 8: The chromatograph of HPLC for p-xylene.

CONCLUSIONS

In this study, Graphene nanosheets (GNS) were surveyed to assess its capacity to remove p-xylene from aqueous solution. It was found that removal capacity is about 81 % with contact time of 180 min between GNS and solution of p-xylene. GNS exhibited favorable adsorption isotherm as well as faster kinetics, and the experimental data of adsorption were best followed by the Langmuir model for isotherm and pseudo-first order model for the kinetics. GNS had also displayed high affinities to p-xylene organic compound, dominated by π–π interactions to the flat surface and the sieving effect of the powerful groove regions formed by wrinkles on GNS surfaces. Thermodynamic study showed that p-xylene adsorption onto the adsorbent was physical, endothermic and spontaneous. As tested in this study, GNS exhibited better adsorption capacities than carbon nanotubes for p-xylene removal, and favorable adsorption of GNS compared to CNT was also consistent with the order of specific surface area and pore volume. It was shown that, only a small amount of GNS is needed in order to achieve the removal of p-xylene from aqueous solution, may be due to the large interfacial area and high aspect ratio of GNS. Given the above promising results from GNS, it can be concluded that wastewater treatment is one of the most promising application areas of GNS, which are not only superior to CNT but also less expensive for large-scale manufacturing, so it may be possible to utilize these alternative nanomaterials in wastewater treatment more in the near future, hoping to improve the quality of water that constitute a major source of life. The results are important to understand the possible application of graphene nanomaterials in environmental pollution management.

ACKNOWLEDGMENTS

REFERENCES

[1]   Botalova O, Schwarzbauer J, Frauenrath T, Dsikowitzky L. Water Res 2009; 43: 3797-3812.
[2]   Jo MS, Rene ER, Kim SH, Park HS. J Hazard Mater 2008; 152: 1276-1284.
[3]   Santos KAO, Dantas Neto AA, Moura MCPA, Castro Dantas TN. Brazil J Petro Gas 2011; 5: 255-268.
[4]   Moura CP, Vidal CB, Barros AL, Costa LS, Vasconcellos LCG, Dias FS, Nascimento RF. J Colloid Interface Sci 2011; 363: 626-634.
[5]   Vidal CB, Raulino GSC, Barros AL, Lima ACA, Ribeiro JP, Pires MJR, Nascimento RF. J Environ Manage 2012; 112: 178-185.
[6]   Wu H, Wang L, Zhang J, Shen Z, Zhao J. Catal Commun 2011; 12: 859-865.
[7]   Farhadian M, Duchez D, Vachelard C, Larroche C. Water Res 2008; 42: 1325-1341.
[8]   Lillo-Ródenas MA, Cazoria-Amorós D, Linares-Solano A. Carbon 2005; 43: 1758-1767.
[9]   Novoselov KS, Geim AK, Morozov SV, Jiang D, Zhang Y, Dubonos SV, Grigorieva IV, Firsov AA. Science 2004; 306: 666-669.
[10]   Deng X, Lü L, Li H, Luo F. J Hazard Mater 2010; 183: 923-930.
[11]   Stankovich S, Dikin DA, Piner RD, Kohlhaas KA, Kleinhammes A, Jia Y, Wu Y, Nguyen ST, Ruoff RS. Carbon 2007; 45: 1558-1565.
[12]   Agnihotri S, Rood MJ, Rostam-Abadi M. Carbon 2005; 43: 2379-2388.
[13]   Li L, Chen W, Xu Z, Zheng S, Zhu D. J Environ Qual 2013, 42: 191-198.
[14]   Geim AK, Novoselov KS. Nat Mater 2007; 6: 183-191.
[15]   Geim AK. Science 2009; 324: 1530-1534.
[16]   Pei Z, Li L, Sun L, Zhang S, Shao X, Yang S, Wen B. Carbon 2013 51: 156-163.
[17]   Xu J, Wang L, Zhu Y. Langmuir 2012; 28: 8418-/8425.
[18]   Febrianto J, Kosasih AN, Sunarso J, Ju Y, Indraswati N, Ismadji S. J Hazard Mater 2009; 162: 616-645.
[19]   Langmuir I. J Amer Chem Soc 1916; 38: 2221-2295.
[20]   Freundlich H. J Phys Chem 1906 57: 385-470.
[21]   Sips R. J Chem Phys 1948; 16: 490-495.
[22]   Chin CJ, Shih LC, Tsai HJ, Liu TK. Carbon 2007; 45: 1254-1260.
[23]   Mangun CL, Yue Z, Economy J. Chem Mater 2001; 13: 2356-2360.
[24]   Wibowo N, Setyadhi L, Wibowo D, Setiawan J, Ismadji S. J Hazard Mater 2007; 146: 237-242.
[25]   Lagergren S, Sven K. Kungliga Svenska Vetenskapsakad Handl 1898; 24: 1–39.

[26]   Ho YS. Adsorption of heavy metals from waste streams by peat. University of Birmingham, Birmingham, 1995.
[27]   HO YS, McKay G. Process Biochem 1999; 34: 451-465.
[28]   Lazar P, Karlicky F, Jurečka P, Kocman M, Otyepkova E, Šafářova K, Otyepka M. J Am Chem Soc 2013; 135: 6372.
[29]   Pan B, Lin D, Mashayekhi H, Xing B Environ Sci Technol 2008; 42: 5480.
[30]   Glukhova O, Slepchenkov M. Nanoscale 2012; 4: 3335.
[31]   Meyer JC, Geim AK, Katsnelson MI, Novoselov KS, Booth TJ, Roth S. Nature 2007; 446: 60.
[32]   Fasolino A, Los JH, Katsnelson MI. Nat Mater 2007; 6: 858.
[33]   Anandkumara J, Mandal B, J Hazard Mater 2009; 168: 633.